JOURNAL OF MATERIALS SCIENCE **41** (2006) 13–25

Factors influencing the piezoelectric behaviour of PZT and other "morphotropic phase boundary" ferroelectrics

ANDREW J. BELL
Institute for Materials Research, University of Leeds, UK

Recent studies of the mechanism of piezoelectricity in PZT and related materials are reviewed and complemented by new analyses based on the Landau-Ginzburg-Devonshire theory of ferroelectricity. Particular attention is given to the nature of the morphotropic phase boundary between the tetragonal and rhombohedral perovskite phases and the accompanying peak in the piezoelectric coefficient. The importance of the changes in angular dependence of single crystal piezoelectric coefficients as a function of composition is highlighted together with the concept of field-induced rotation of the polarization in the (110) plane. It is shown that introducing the tendency to form monoclinic phases enhances this phenomenon.
The model that the monoclinic phase in PZT is due to the condensation of local disorder in the polar cation displacements from the macroscopic tetragonal and rhombohedral phases is examined in some detail using statistical analyses of the Zr/Ti conformation. Whilst the concept of monoclinic nano-domains is not inconsistent with statistically random distributions, it is argued that some ordering of the B-site cations may be required to enable the transformation to a macroscopically observable phase. The implications of this model on the contribution of polarization rotation to piezoelectricity in PZT are discussed.

1. Introduction

Lead zirconate titanate ($PbZr_{1-z}Ti_zO_3$ or PZT) has been the leading, high activity piezoelectric material for over 40 years and consequently is at the heart of the majority of piezoelectric actuators and sensors in production today [1]. However, in response to the introduction of environmental legislation, aimed at reducing the quantities of heavy metals entering the environment, research into alternative, lead-free piezoelectric materials is currently accelerating [2].

For the majority of applications of PZT, the optimum performance is found at the boundary between the tetragonal and rhombohedral perovskite phases (see Fig. 1), often known as the morphotropic phase boundary (MPB) [1]. Conventional wisdom suggests that for compositions close to the MPB, the piezoelectric coefficients maximise due to (i) a peak in the spontaneous polarization, to which the intrinsic piezoelectric coefficient is proportional and (ii) near degeneracy of the tetragonal and rhombohedral states, which allows for ease of reorientation of domains under applied fields and stresses, thereby maximising the extrinsic piezoelectric contributions. Consequently, much of the past research and development work on PZT has focused on the management of domain wall mobility through the control of defect chemistry. The discussions in this paper, however, focus mainly on the intrinsic contribution.

Since the morphotropic phase boundary in PZT ceramics is seen as central to their outstanding piezoelectric performance, the search for new or improved materials focuses on systems which possess a similar phase boundary. However, a number of relatively recent discoveries have driven a reassessment of our understanding of the MPB in PZT; these are:

(i) The unprecedented performance of complex-perovskite single crystals, such as [001]-oriented $Pb(Zn_{1/3}Nb_{2/3})O_3$-$PbTiO_3$ compositions on the rhombohedral side of their MPB; the mechanism appears to rely

0022-2461
DOI: 10.1007/s10853-005-5913-9

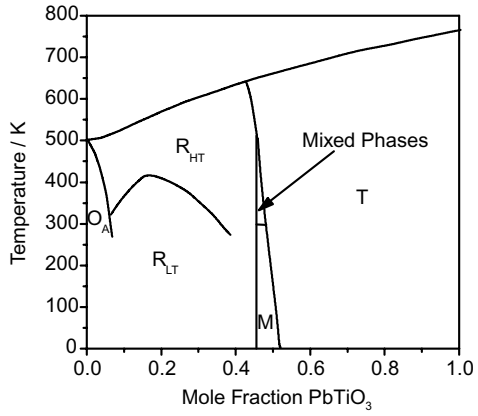

Figure 1 The phase diagram of $Pb(Zr_{1-z}Ti_z)O_3$ modified from Jaffe, Cook and Jaffe [1] to include the monoclinic phase [4].

on a field-induced rotation of the polarization vector in the (110) plane from the [111] to the [001] axis [3].

(ii) A previously undetected monoclinic phase at the morphotropic phase boundary in PZT [4] with polarization in the (110) plane and the presence of monoclinic [5] and orthorhombic [6] phases at the phase boundary in the complex-perovskites;

(iii) The local atomic displacements in PZT appear to differ from those consistent with the macroscopic symmetry [7]: for example, in the rhombohedral phase the lead cation displacements seem to be composed of local, short-range, random arrangements of tetragonal type displacements superimposed on the average, long range rhombohedral order.

This paper explores these findings, with an emphasis on using thermodynamic and statistical models to help understand how the anomalous piezoelectric properties close to the MPB arise.

2. Polarization rotation

A simplistic treatment of the intrinsic component of piezoelectricity might suggest that the piezoelectric effect is greatest parallel to the polar axis. That is, on applying an electric field parallel to the spontaneous polarization, P_s, it is augmented by an induced polarization, P_{ind}, which adds to the lattice strain, x:

$$\begin{aligned} x &= Q\,(P_s + P_{ind})^2 \\ &= Q P_s^2 + 2Q P_s P_{ind} + Q P_{ind}^2 \approx x_s + 2Q P_s P_{ind} \\ &\Rightarrow \Delta x \approx 2Q P_s \varepsilon E \end{aligned} \tag{1}$$

where x_s is the spontaneous strain and Q is the relevant electrostriction coefficient. For small fields, the induced strain, Δx, is proportional to the electrostriction coefficient, the spontaneous polarisation and the permittivity, ε, where E is the applied electric field; the approximation for high permittivity materials, $\varepsilon \approx \frac{dP}{dE}$, is implicit. Hence the intrinsic piezoelectric coefficient, d_{int}, is given by

$$d_{\text{int}} = 2Q P_s \varepsilon. \tag{2}$$

As the direction of P_s is normally taken to be the direction of maximum spontaneous polarisation, this textbook treatment can lead to the fallacy that the maximum intrinsic piezoelectric effect occurs parallel to the polar axis. Whilst this may be true for simple compounds well removed from phase transitions, it does not necessarily hold close to phase transitions at which the direction of the spontaneous polarization changes (for example at the morphotropic phase boundary in PZT or at the tetragonal-orthorhombic transition in barium titanate).

The misconception is highlighted by the large piezoelectric effect in "domain-engineered" complex perovskite single crystals [3]. It was noted that close to the MPB, in [001]-poled rhombohedral crystals, the piezoelectric coefficient is much greater parallel to [100] than it is along the polar [111] axis. It was proposed and confirmed [8] that on applying a field parallel to [001], the polarization rotated from the [111] axis continuously through the (110) plane to lie parallel, at a sufficiently high field, to the [001] axis. This "polarization rotation" was accompanied by a large induced strain. Support for this type of mechanism came in the form of calculations, from both the *ab initio* [9] and thermodynamic [10] schools, using $BaTiO_3$ as a prototype. In the latter case, the Landau-Ginzburg-Devonshire (LGD) approach [11] was used to show how the piezoelectric coefficients parallel to the non-polar low-index axes could exceed those parallel to the zero-field polar axes, again due to field induced rotation of the polarization vector. Furthermore, Damjanovic [12] calculated that in barium titanate the direction of maximum piezoelectric coefficient itself rotates as a function of temperature close to the tetragonal-orthorhombic transition. A number of *ab initio* calculations for PZT have also supported the rotation hypothesis [13, 14].

Whilst "polarization rotation" has been observed experimentally in complex perovskite crystals [8] and to a certain extent in barium titanate crystals [15], it is pertinent to ask how important is it in PZT ceramics and what is the role of the monoclinic phase?

3. LGD theory

The conventional Landau-Ginzburg-Devonshire model of ferroelectrics [11] as applied to perovskites is based on an elastic Gibbs' free energy expansion. In the stress-free case it is of the form:

$$\begin{aligned} \Delta G = {} & \alpha_{200}\left(P_1^2 + P_2^2 + P_3^2\right) + \alpha_{400}\left(P_1^4 + P_2^4 + P_3^4\right) \\ & + \alpha_{220}\left(P_1^2 P_2^2 + P_2^2 P_3^2 + P_3^2 P_1^2\right) + \alpha_{600}\left(P_1^6\right. \\ & \left. + P_2^6 + P_3^6\right) + \alpha_{420}\left(P_1^4 P_2^2 + P_1^2 P_2^4 + P_2^4 P_3^2\right. \end{aligned}$$

$$+ P_2^2 P_3^4 + P_3^4 P_1^2 + P_3^2 P_1^4) + \alpha_{222} P_1^2 P_2^2 P_3^2 - E_1 P_1 - E_2 P_2 - E_3 P_3 \quad (3)$$

Here the series is terminated arbitrarily at the sixth power of polarization. P_i are the orthogonal components of polarization measured parallel to the pseudo-cubic axes of the perovskite unit cell. E_i are the corresponding components of the applied electric field. The coefficient α_{200} is necessarily temperature dependent. Hence, providing that the values of all the α_{lmn} coefficients are known, the values of the components of polarization can be determined for any combination of temperature and applied field by minimization of ΔG. Although zero-field analytical solutions exist, generally, and particularly for the case of non-zero fields, solutions are more easily found numerically.

The lattice strains are given by:

$$x_{ij} = Q_{ijkl} P_k P_l \quad (4)$$

where **Q** is the electrostriction tensor.

For an arbitrary direction of electric field of amplitude E_0 and direction θ to the [001] axis and ϕ in the [110] plane, the polarization vector, **P**, and strain tensor, **x**, can be determined. Appropriate transformations can be applied to calculate the induced strain and piezoelectric coefficient $d_{\theta\phi}$ parallel to the direction of the field, using:

$$\begin{aligned} E_1 &= E_0 \sin\theta \cos\phi \\ E_2 &= E_0 \sin\theta \sin\phi, \\ E_3 &= E_0 \cos\theta \end{aligned} \quad (5)$$

$$x_{\theta\phi} = x_3 \cos^2\theta - \cos\theta \sin\theta (x_6 \cos\phi + x_5 \sin\phi) + \sin^2\theta (x_1 \cos^2\phi - x_4 \cos\phi \sin\theta + x_2 \sin^2\phi) \quad (6)$$

and

$$d_{\theta\phi} = \frac{x_{\theta\phi}(E_0) - x_{\theta\phi}(0)}{E_0}, \quad (7)$$

where x_i represents elements of the strain tensor, according to the reduced notation convention [16] and $x_{\theta\phi}$ is the strain parallel to the applied field.

The set of coefficients, α_{lmn}, are dependent upon titanium concentration, z. The set employed throughout this paper, is adapted from the coefficients proposed by Haun [17, 18] and are shown in Table I. The value of α_{200} is for a temperature of 300 K. The present calculations are simplified by treating $PbZrO_3$ as a rhombohedral ferroelectric rather than an orthorhombic antiferroelectric. By extrapolation of the Haun coefficients in the rhombohedral phase of PZT to zero titanium content, a set of coefficients for $PbZrO_3$ were derived that satisfy this hypothetical scenario. To provide greater resolution close to the MPB, the coefficients for $0.4 < z < 0.6$ were fitted to fourth order polynomials in z, allowing calculations to be made for any value of titanium concentration in this range.

Fig. 2 shows results for the angular dependence of the piezoelectric coefficient, $d_{\theta\phi}$, from the numerical calculations under weak field conditions ($E_0 = 1000\ \mathrm{V\ m^{-1}}$). The data (excluding $PbZrO_3$) are identical to those of reference [19] obtained by analytical methods. It can be seen that for the end-members of the solid solution, $PbTiO_3$ and the fictitious, rhombohedral ferroelectric $PbZrO_3$, the maximum induced strain is indeed parallel to the polar axis, i.e. along [001] and [111] respectively. However, even for moderate levels of B-site substitution the direction of maximum strain shifts. In rhombohedral $Pb(Zr_{0.6}Ti_{0.4})O_3$, the direction of maximum strain is clearly along <100>, whilst in tetragonal $Pb(Zr_{0.4}Ti_{0.6})O_3$, the strain has become more isotropic than in $PbTiO_3$. The significance of such calculations is confirmed by experimental data for PZT thin-films: the piezoelectric coefficients of [001]-oriented, rhombohedral films is almost twice that of [111]-oriented films of the same composition [20] indicating that the non-polar [001] direction has the larger piezoelectric coefficient.

Although the LGD model suggests that on approaching the MPB the direction of maximum piezoelectric activity moves away from the polar axis, in this form it does not necessarily identify polarization rotation as being the dominant mechanism of piezoelectricity. For instance, calculations of the field-induced strain along [001] for rhombohedral compositions near the MPB [21] under high field, suggest a discontinuous polarisation switching between the [111] and [001] directions, that is a first-order field-induced transition. This is contrary to the experimental evidence for complex-perovskites which suggest a continuous polarization rotation mechanism, consistent with a second order transition [8].

4. Monoclinicity

The discovery that there exists a monoclinic phase in PZT, intermediate to the tetragonal and rhombohedral phases at the MPB [4], reveals that the 6th order Landau model used for the above calculations is flawed, in that it does not admit solutions for phases in which non-zero components of polarization can be unequal, as is the case in monoclinic phases. Subsequently it has been shown that thermodynamic functions allowing monoclinic and triclinic solutions require terms up to the 8th and 12th order respectively [22]. The inclusion of the higher order terms in the free energy expansion not only allows a monoclinic phase, but for tetragonal and rhombohedral ground states can encourage monoclinicity, that is rotation of the polarization vector in the (110) plane, under applied fields of the type identified in the complex perovskite single crystals. Revision of the Haun model to include higher or-

TABLE I 6th order free energy coefficients for $Pb(Zr_{1-z}Ti_z)O_3$

					Interpolation for $0.4 < z < 0.6$									
z	0.0	0.1	0.2	0.3	z^0	z^1	z^2	z^3	z^4	0.7	0.8	0.9	1.0	Multiplier
α_{200}	−4.582	−6.376	−7.47	−8.116	830.65	−7034.2	+21670	−29020	+14263	−12.47	−14.84	−16.17	−1.708	$\times 10^7$
α_{400}	52.35	41.25	31.29	22.3	−1161.4	+10056	−31486	+42802	−21443	0.6458	−3.05	−5.845	−7.9	$\times 10^7$
α_{220}	−16.71	−4.22	−0.0345	1.688	−366.50	+3070.4	−9447.1	+12716	−6313.8	5.109	6.32	7.063	7.5	$\times 10^8$
α_{600}	5.932	5.068	4.288	3.56	−287.77	+2452.1	−7617.7	+10307	−5141.2	2.348	2.475	2.518	2.61	$\times 10^8$
α_{420}	311.2	34.45	18.14	15.27	−1365.4	+11613	−36026	+48732	−24309	10.25	9.684	8.099	6.3	$\times 10^8$
α_{222}	−104.1	−8.797	−7.545	−7.052	647.96	−5506.9	+17075	−23090	+11514	−5.003	−4.901	−4.359	−3.66	$\times 10^9$

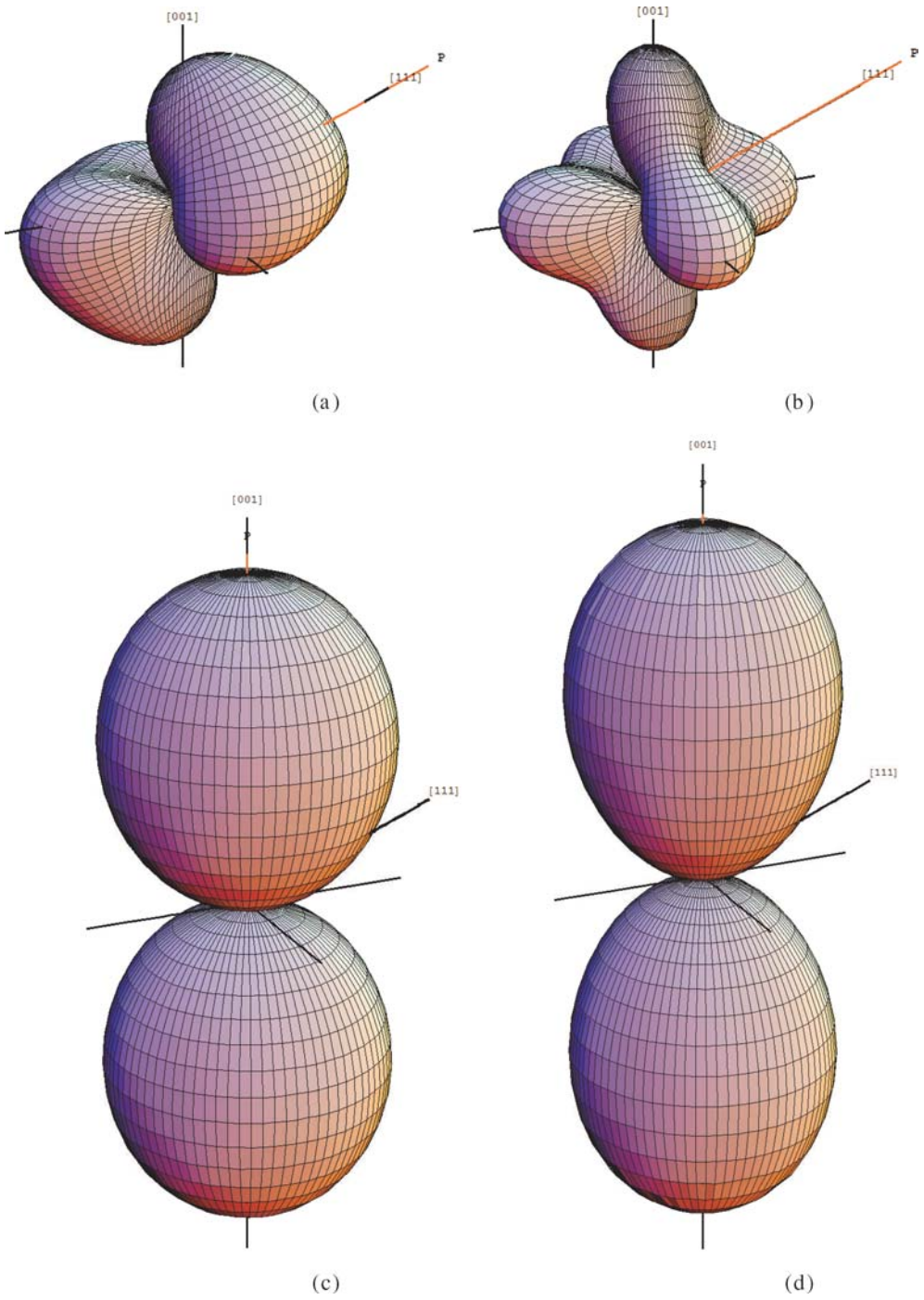

Figure 2 Single crystal piezoelectric coefficient as a function of angle, $d_{\theta\phi}$, for $Pb(Zr_{1-z}Ti_z)O_3$ from the 6th order LGD model: (a) $z = 0$, (b) $z = 0.4$, (c) $z = 0.6$ and (d) $z = 1$.

der terms can demonstrate how polarization rotation may be responsible for exceptional piezoelectric properties.

The additional terms for the expansion up to the eighth power of polarization are:

$$\Delta G = \ldots + \alpha_{800}\left(P_1^8 + P_2^8 + P_3^8\right) + \alpha_{620}\left(P_1^2\left(P_2^6 + P_3^6\right) + P_2^2\left(P_3^6 + P_1^6\right) + P_3^2\left(P_1^2 + P_2^2\right)\right) + \alpha_{440}\left(P_1^4P_2^4 + P_2^4P_3^4 + P_3^4P_1^4\right) + \alpha_{422}\left(P_1^4P_2^2P_3^2 + P_1^2P_2^4P_3^2 + P_1^2P_2^2P_3^4\right)$$

Fig. 3 shows a contour plot of ΔG for $PbZr_{0.55}Ti_{0.45}O_3$ in the (110) plane for the 6th order set of coefficients of Table I. The x-axis represents the value of the polarization along [110] with $P_1 = P_2$, whilst the y-axis is P_{001} $(= P_3)$.

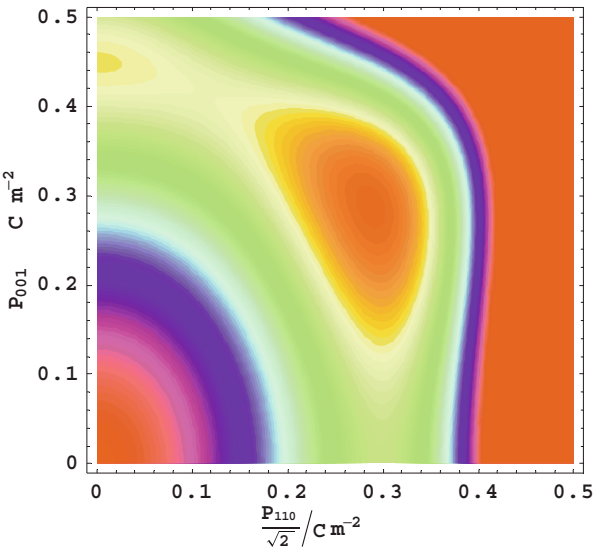

Figure 3 Contour plot of free energy as a function of polarization in the [110] plane for $Pb(Zr_{0.55}Ti_{0.45})O_3$ from the sixth-order LGD model. The energy at point {0,0} is 0 J m^{-3}; the minimum occurs at point {0.29, 0.29} with an energy of -8.06×10^6 J m^{-3}; contours occur at intervals of 8×10^4 J m^{-3}.

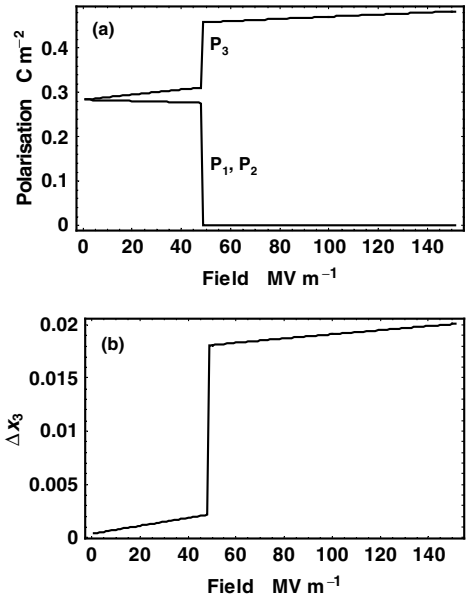

Figure 4 (a) Polarization and (b) strain as a function of applied field for $Pb(Zr_{0.55}Ti_{0.45})O_3$ from the sixth order LGD model.

In such plots a minimum lying on the *y*-axis represents tetragonal symmetry. A minimum on the *x*-axis indicates that an orthorhombic phase is stable, whilst a minimum on the line $P_{110} = P_{001}$ indicates a rhombohedral phase. Minima at any other points in the plane are of monoclinic symmetry. In this plot, the energy is zero at $P_{110} = P_{001} = 0$ and is positive for $P_{110} > 0.4$. All other values are negative. The absolute minimum can be seen to be at $P_{110} = P_{001} = 0.29$, indicating a rhombohedral phase is stable. A secondary minimum is seen at the point $\{P_{110}, P_{001}\} = \{0, 0.43\}$. However, there is a significant energy barrier between the 2 states, indicating that although a sufficient field parallel to [001] may result in the tetragonal phase becoming stable, the transition will occur via a discontinuity in the polarization as the barrier is traversed. This is demonstrated in Fig. 4a and b which show the components of polarization and strain calculated as a function of applied field along [001] for the same example. To demonstrate the concept of monoclinicity, a set of 8th order coefficients ('A' in Table II) have been derived.

In general the 8th order coefficients in the LGD expansion are expected to be relatively small. In principle they can be derived experimentally by fitting of the $P(E)$ characteristic to the LGD model for a single crystal sample. At present this is not possible for PZT, for which good examples of single crystals are notably rare. Alternatively, the 8th order coefficients can be estimated by fitting the temperature dependence of the lattice parameters to the LGD model. However, the accuracy of this method is expected to be poor unless the data encompasses a transition to the monoclinic state, which cannot be modelled without the 8th order terms. Hence the 8th order terms could be derived for that range of compositions exhibiting a monoclinic phase and for which could crystallographic is available [4]. The approach taken here is to employ 8th order coefficient values which are the minimum necessary to illustrate the effects in question.

Although coefficient set 'A' does not stabilize the monoclinic state at zero field, the tendency towards monoclinic symmetry is signalled by the removal of the energy barrier between the rhombohedral and tetragonal phases. Figs 5 and 6 illustrate this with free energy contour plots for the 8th order case. In Fig. 5, at zero field, the absolute minimum in energy is close to the point {0.26, 0.26}. However, there is a rather flat-bottomed valley connecting this point to the "tetragonal" point on the *y*-axis. This represents the easy path for rotation of the polarization. On applying a field along [001], the minimum moves continuously along this path. As an example Fig. 6 shows the plot for $E_3 = 5$ MV m^{-1} in which the minimum has shifted to the point {0.19, 0.37}. Again this is emphasised with plots of polarisation and strain as a function field (Fig. 7a and b). The path of the induced strain is similar to that seen in single crystal complex-perovskites [3]. Thus, under applied fields, the material passes through an extended region of monoclinic stability, corresponding

TABLE II Additional 8th order free energy coefficients for $Pb(Zr_{1-z}Ti_z)O_3$

	A	B
α_{222}	-2×10^9	as Table I
α_{800}	5×10^8	0
α_{620}	-2×10^9	-2.5×10^9
α_{440}	4×10^9	5×10^9
α_{422}	0	0

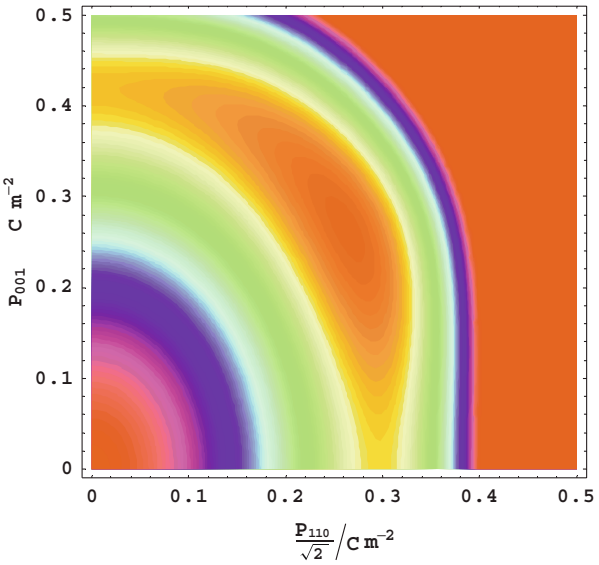

Figure 5 Contour plot of free energy as a function of polarization in the [110] plane for $Pb(Zr_{0.55}Ti_{0.45})O_3$ from the eighth-order LGD model. The energy at point {0,0} is 0 J m^{-3}; the minimum occurs at point {0.26, 0.26} with an energy of -7.05×10^6 J m^{-3}; contours occur at intervals of 7×10^4 J m^{-3}.

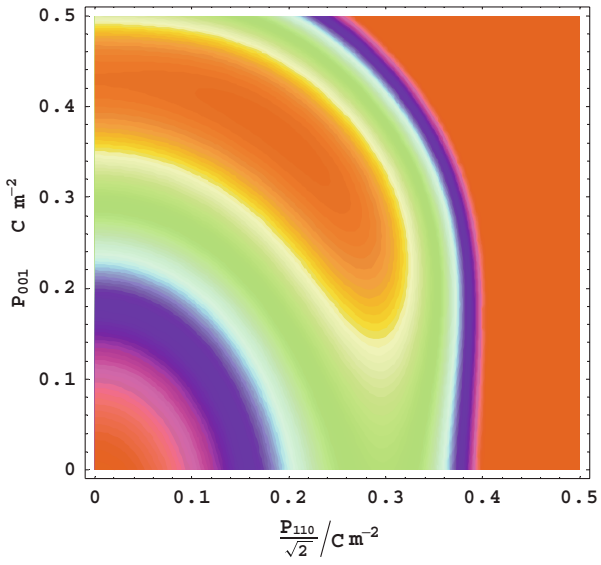

Figure 6 Contour plot of free energy as a function of polarization in the [110] plane for $Pb(Zr_{0.55}Ti_{0.45})O_3$ from the eighth-order LGD model for a field of 5×10^6 V m^{-1} applied parallel [001]. The energy at point {0,0} is 0 J m^{-3}; the minimum occurs at point {0.19, 0.37} with an energy of -8.6×10^6 J m^{-3}; contours occur at intervals of 9×10^4 J m^{-3}.

to rotation of the polarization vector in the (110) plane. These states are not accessible in the 6th order model. Although the high-field strain calculated under the 8th order model is slightly lower than the 6th order predictions, the weak field piezoelectric coefficient, i.e. the slope of the strain-field curves, is much larger when significant polarisation rotation is permitted. The fields employed for these simulations are consistent with those providing experimental for the complex perovskites.

It should be stressed that the coefficients listed in Table II do not necessarily represent a self-consistent set of free-energy coefficients, but have been selected purely to illustrate the concepts under discussion.

Fig. 8 shows $d_{\theta\phi}$ for $Pb(Zr_{0.4}Ti_{0.6})O_3$ at 300 K for the same set of additional 8th order coefficients. For these coefficients there is no stable monoclinic form in the zero-field phase diagram, but as can be seen by comparison with Fig. 2c, the set has a profound influence on $d_{\theta\phi}$. Although the response is still consistent with tetragonal symmetry, the maximum in piezoelectric coefficient lies away from the polar direction, its locus being in the form of a circle about the [001] axis and including the [111] direction.

The calculation of $d_{\theta\phi}$ can provide an estimate of the piezoelectric coefficient of a poled ceramic parallel to the poling direction, d_p, by averaging $d_{\theta\phi}$ over the appropriate range of angles. Fig. 9a compares the values of d_p close to the MPB, taking into account either tetragonal or rhombohedral phase poling, for the Haun model and for the 8th order coefficient set A. The greater freedom for polarization rotation provided by the 8th order terms results in a significant increase in piezoelectric coefficient. Fig. 9b

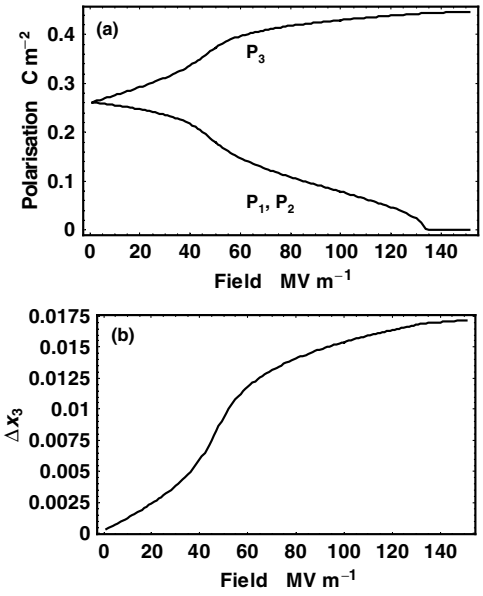

Figure 7 (a) Polarization and (b) strain as a function of applied field for $Pb(Zr_{0.55}Ti_{0.45})O_3$ from the eighth-order LGD model.

shows the results of the same calculation for coefficient set B. This set of 8th order coefficients has been selected to illustrate the stabilisation of a monoclinic phase at the MPB phase, over a range similar to that observed experimentally [4]. The magnitude of piezoelectric coefficient is greater than experiment suggests, but the data may account better for the sharp divergence of the piezoelectric properties at the MPB [1] than do other models. For com-

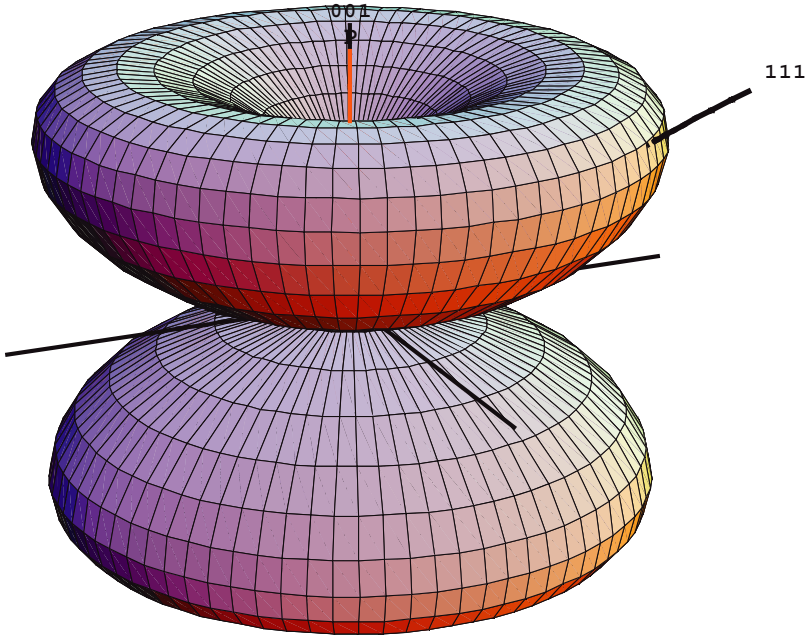

Figure 8 Single crystal piezoelectric coefficient as a function of angle, $d_{\theta\phi}$, for $Pb(Zr_{0.4}Ti_{0.6})O_3$, calculated from the 8th order LGD model using coefficient set A.

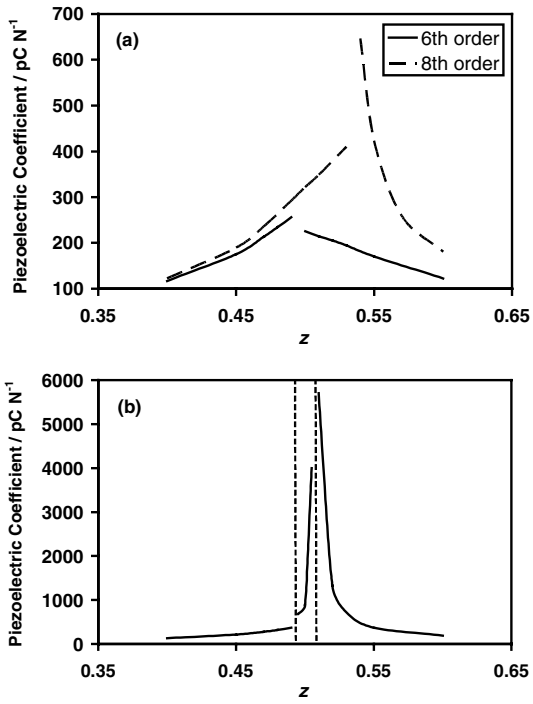

Figure 9 Piezoelectric coefficients as a function of titanium concentration calculated for poled ceramics from the LGD model employing (a) the 6th order and 8th order model (coefficient set A) and (b) the 8th order model (coefficient set B).

parison, $d_{\theta\phi}$ calculated for monoclinic $Pb(Zr_{0.5}Ti_{0.5})O_3$ from coefficient set B, is shown in Fig. 10.

The above examples give weight to the argument that monoclinicity, the capacity of a crystal to be stable in monoclinic forms over significant regions of parameter space, (although not necessarily at zero-field), is important in increasing piezoelectric activity by allowing the rotation of the polarisation vector in the (110) plane.

5. Monoclinic nanodomains

There is strong evidence that the monoclinic motif is present in PZT over a wide range of titanium concentration, not only in the region of the MPB. From structure refinements of neutron diffraction data [9] it appears that the "local symmetry," as indicated by the shift of the Pb-ions from the cubic setting, might best be described as monoclinic in both the rhombohedral and tetragonal phases. These suggestions were prompted by the observation that in the structure refinement process, if the cation displacements are constrained along directions which are consistent with the assumed macroscopic symmetry, the temperature factors associated with these displacements appear to be unreasonably large in directions perpendicular to the displacement. Temperature factors are normally expected to be spherically symmetric about the lattice position of the ion with which they are associated. To eliminate the anisotropy, without compromising the quality of the refinement, "off-axis" cation displacements are introduced, i.e. Pb ions may displace in directions other than [111] in the rhombohedral phase or [001] in the tetragonal phase. Thus, a static model structure which fit the data was identified: in the rhombohedral phase [9], the displacement of the Pb-ions from their cubic position comprises a long-range ordered, homogeneous [111] displacement, superimposed with lo-

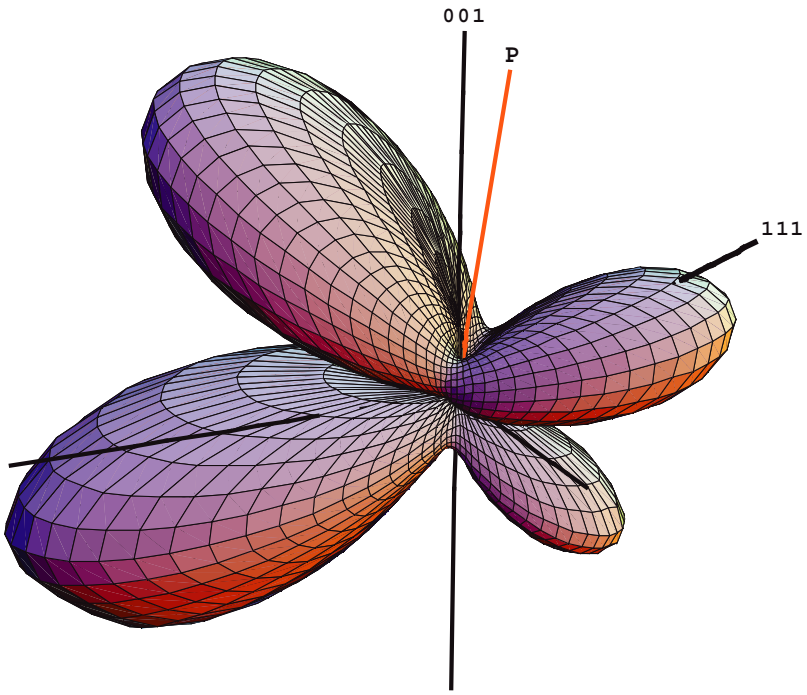

Figure 10 Single crystal piezoelectric coefficient as a function of angle, $d_{\theta\phi}$, for $Pb(Zr_{0.5}Ti_{0.5})O_3$, calculated from the 8th order LGD model using coefficient set B.

cal, randomly oriented, minor <001> shifts. Frantti [23] applied the same arguments to data for the tetragonal phase, proposing that homogeneous [001] cation displacements are augmented with minor <110> (or possibly <111>) randomly oriented shifts. In both cases, the random shifts average to zero so that the macroscopic symmetries remain rhombohedral and tetragonal, respectively.

Bell and Furman postulated [24] that the macroscopic monoclinic phase may be due to condensation of the short-range random displacements into longer range ordered structures and proposed a mixed-crystal LGD model to describe this concept [25]. This concept has been more thoroughly explored independently by Glazer [26]. Working from the hypothesis that the monoclinic phase at the MPB was due to a change in coherence length of the monoclinic nano-domains that constitute the "rhombohedral" and "tetragonal" phases, it was concluded that for structure probes with sufficiently fine coherence length the morphotropic phase boundary does not exist.

First principles calculations [27, 28] tend to support the model of local monoclinic symmetry. DFT calculations carried out on 8 and 6 unit supercells showed that the Pb-ion displacements can be perturbed from the macroscopic polar direction by the particular conformation of nearest neighbour Ti and Zr ions, with resultant local polar displacements that need not conform to [001] or [111]. The implication is that for random placements of Zr and Ti on the B-site sub-lattice, there is disorder in the Pb displacements similar to those in the Glazer model [26].

The A-site cation response to the B-site disorder in PZT can be traced to the geometry of the Pb-O bonding of the end-members [29]. The fact that $PbTiO_3$ and $PbZrO_3$ tend to adopt different structures, may be attributed to the fact that PbO itself is polymorphic with an α-form exhibiting pyramidal Pb-O motifs of high geometric stability. In this conformation, the Pb lone-pair takes up a position opposite to the square oxygen base of the pyramid. An almost identical Pb-O arrangement is also present in $PbTiO_3$. However, β-PbO contains a trigonal bi-pyramidal Pb-O arrangement with less intrinsic stability, vestiges of which can be found in the structure of $PbZrO_3$. Local disorder in PZT may therefore be interpreted as the strong tendency of $PbTiO_3$ to form square pyramid Pb-O groups being frustrated by the destabilising influence of the Zr additions. Hence ambivalence in the oxygen coordination of the polar ion, combined with the presence of a lone pair can facilitate polar displacement disorder.

It is tempting to extend these arguments to cover known monoclinic type phases in the complex perovskite MPB systems. However, for these materials, an almost diametrically opposite model has been proposed [30], in which it is suggested that for domains with low wall energies, nanodomain structures of local tetragonal symmetry occur, which appear monoclinic when examined with long correlation length probes.

6. Monoclinic fluctuations

The main experimental evidence for the Glazer model comes from the relaxation of constraints on cation displacements employed to avoid the appearance of highly anisotropic temperature factors in structure refinements. The possibility of anisotropic dynamic fluctuations was suggested to be unphysical [7], but with little justification. It is therefore relevant to examine this suggestion in more detail.

The permittivity of ferroelectrics is generally highly anisotropic; perpendicular to the polar axis it is much larger than it is parallel to it. The permittivity is a measure of the ease of displacement of charge by an electric field imposed on the system and in the case of PZT appears to be dominated by the polarizability of the Pb ion. Any anisotropy observed in permittivity is hence a consequence of anisotropy in the free energy and a reflection of the anisotropy of the potential well for the Pb ion. Given the dominant role of Pb in PZT, it can be argued that the free energy landscape, as portrayed in Fig. 5, is an approximation of the potential seen by the Pb ions. Hence, thermal fluctuations within such a potential would be highly anisotropic and, given the broad flat nature of the well in the arc between [110] and [001], would be expected to be much larger than parallel to [111]. Hence it may not be so unusual for there to be significant, or even anomalous, dynamic fluctuations of the polar cations approximately perpendicular to the polar direction, producing the type of temperature factors seen in the constrained structure refinements. Indeed, extrapolating from Fig. 5 into three dimensions would suggest that any dynamic fluctuations observed would be constrained to a dish-shaped region with its symmetry axis lying along the [111] axis, similar in form to those described by Corker [7].

In this alternative model, the local symmetry at any instant in time would still appear monoclinic, but with temporal rather than spatial fluctuations of the Pb ion about the polar axis. Hence, the macroscopic monoclinic phase observed at the MPB would be interpreted as an ordering and freezing-in of these fluctuations, rather than a growth in the coherence length of static displacements.

Given the evidence from the *ab initio* calculations that the Pb displacements are strongly dependent upon the local Zr/Ti conformation, it would appear that the static interpretation of local random displacements is the more likely, although dynamic fluctuations may play a role.

Independent of whether the static or dynamic model offers the more accurate description of the structure, the common feature is a unit cell which is essentially monoclinic across the phase diagram. It is the scale of its correlation in space and time which determines the macroscopically observed phase. It is therefore pertinent to ask why the coherence of the local monoclinic structures should become macroscopic near the MPB?

7. Statistics of the Zr/Ti distribution

To understand this aspect of the problem, an exploration of the statistics of the Zr/Ti conformation is useful, especially in view of the rather small sample sizes considered in the *ab initio* studies [28]. The Zr/Ti distribution in PZT is, to date, believed to be totally random. A simple Monte Carlo type model has been constructed to determine the average Ti (or Zr) cluster size as a function of the Ti concentration under the assumption of random distributions.

A rigorous determination of cluster size for a 3-dimensional array of random B-site distributions is not a trivial exercise. Here an approximate approach is taken based on the construction of a list of cluster diameters from a 1-dimensional array of random B-site distributions. To construct a representative list of cluster volumes, each member of the list of cluster diameters is multiplied by all members of the list twice. Thus, for a Ti concentration, z, each element in an n-element linear array is populated with a random number r_i which controls the contents of a second array, $\mathbf{u}$: if $r_i < z$, then $u_i = 1$, otherwise $u_i = 0$, representing a Ti unit cell and a Zr unit cell respectively. Examining $\mathbf{u}$ for the number of contiguous occurrences of '1's provides an array of Ti cluster sizes, $\mathbf{s}$. To ensure that the analysis is valid in three dimensions, a list of cluster volumes is derived by flattening the cube of the array, $\mathbf{s} \times \mathbf{s} \times \mathbf{s}$ (i.e. the 3-dimensional array is re-listed as a 1-dimensional array). Although this method provides a distribution of cluster volumes, which approximates to a log normal distribution, to simplify the analysis only the mean of the distribution of cluster volume shall be considered here.

Using the above method, mean cluster volumes were calculated for $z = 0.1$ to 0.9 at intervals of 0.1. In each case, the calculation was carried out for an initial linear array of $n = 500$ unit cells. The resulting 3-dimensional analysis resulted in more than 1 million clusters for z in the range 0.4 to 0.6, and more than 100,000 outside this range. For each value of z, the average of 10 mean cluster volume calculations was determined. The mean cluster volume, v, expressed in unit cells and shown in Fig. 11, fits the surprisingly simple function

$$v = 1/(1 - z)^3. \tag{8}$$

Hence the mean titanium cluster diameter is equal to $1/(1-z)$ unit cells, whilst the mean zirconium cluster size is $1/z$ cells.

The data show that the mean number of contiguous titanium unit cells increases from 1 at vanishingly small concentrations, to just less than 10 at $z = 0.5$, to more than 1000 at $z = 0.9$. Hence, towards the end-members where one of the B-site elements is dominant and Zr/Ti conformation irrelevant, significant volumes of local monoclinic symmetry would seem unlikely. Even in the range $0.4 <$

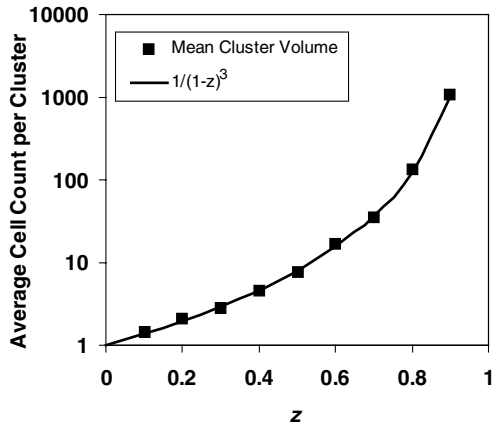

Figure 11 Mean Ti cluster volume calculated as a function of composition for randomly distributed Zr/Ti.

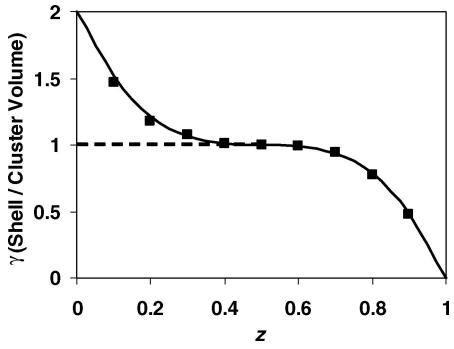

Figure 12 The fraction of the mean cluster volume constituted by surface unit cells as a function of composition.

$z < 0.6$, where the dominant B-site species is expected to have a cluster volume of between 10 and 20 unit cells the effect of B-site conformation might be thought to be minimal and might not conform to Grinberg's *ab initio* calculation [28] in which the assumed cluster sizes are somewhat smaller than 10 unit cells. However, consideration of cluster volumes alone can be misleading; analysis of the most likely nearest neighbour is also necessary. This can be estimated by comparing the number of unit cells at the "surface" of a cluster (i.e. the number of Ti unit cells with at least one Zr nearest neighbour) with the total volume of the cluster. For cuboid clusters of linear dimension l, the number of surface cells, or the volume of the "shell", equates to $l^3 - (l-2)^3$. This is expressed as a shell volume to cluster volume ratio, γ, in Fig. 12, for both the Monte Carlo data and the assumption that $l = 1/(1-z)$. As a result of the assumption of cubic clusters, the relationship is only valid for $l \geq 2$ ($z \geq 0.5$); γ therefore saturates at unity for $z < 0.5$ and relates to the probability of a Ti-cell having a Zr-cell as a nearest neighbour. Representative 2-dimensional arrays of B-site occupancy are shown in Fig. 13 for values of z of 0.5, 07 and 0.9, however these can be misleading as the influence of the third dimension on nearest neighbour probability

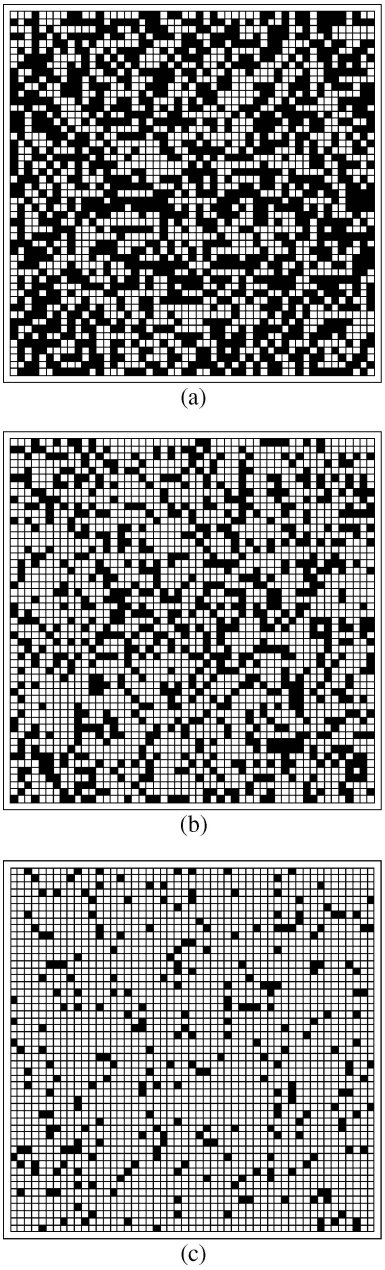

Figure 13 2-dimensional maps of random B-site occupancy for values of z: (a) 0.5, (b) 0.7 and (c) 0.9; Zr occupied cells are shown in black.

is significant and only apparent in the interpretation of Fig. 12. For $z < 0.7$, virtually all Ti-cells have a Zr-cell as a nearest neighbour and it is only for $z > 0.9$ that more than 50% of Ti-cells do not have a Zr neighbour. This treatment therefore shows that for the majority of the phase diagram local Zr/Ti conformations are certainly able to influence the ion displacements in the majority of unit cells and lends further support to the existence of disorder in the local Pb displacements.

The gradual change of the orientation of the polarization with change in Ti concentration requires only that there be chemical disorder on the B-site coupled with the conflict-

ing influences of the two B-site cations on Pb-O bonding. However, the stabilisation of a macroscopic monoclinic phase would seem to require a significant change in the coherence length of these two factors. For the monoclinic phase to appear macroscopic to neutrons and X-rays, the structure should be coherent over at least 0.1 μm [26]. Do the statistics of the Zr/Ti conformation around $z = 0.5$ provide such coherence ? The sum of the mean cluster size of the Zr and Ti clusters is actually a minimum at $z = 0.5$, with the most likely minimum volume in which an equal number of Zr and Ti ions is found being only 16 unit cells (i.e. 1 nm^3). Hence for a neutron-coherent monoclinic region to be observed we should expect some order in the Zr/Ti distribution that transcends the cluster sizes given by random statistics. Given their size difference, positional ordering of the Zr and Ti ions is clearly possible, but it has not yet been reported for PZT.

The two order-parameter LGD model of Bell and Furman [25] predicts a stable monoclinic phase in the region of the MPB, through a coupling of the free energy functions for $PbTiO_3$ and the fictional ferroelectric $PbZrO_3$ of Table I. Whilst this model was proposed as a means of introducing the influence of the disorder in the Zr/Ti distribution into the thermodynamic model, it does not address the issue of coherence length. There is no implication in the results that coherence in the direction of polarization in the monoclinic phase would be observable experimentally. The model was established in the context of the conventional rhombohedral and tetragonal phases being observed at all scale lengths and reflects this. However, it is consistent with the explanation given above for the existence of large anisotropic temperature factors when structure refinements are constrained to these conventional macroscopic symmetries.

8. Piezoelectricity and local structures

What are the implications of the local monoclinic distortions for piezoelectric properties? As demonstrated above, the inclusion of terms in the LGD polarization expansions which tend to stabilize monoclinic symmetry lead to large piezoelectric coefficients due to rotation of the polarization in the [110] plane. However, the calculations which produced Fig. 9, for example, are based on polynomial expansions which are invariant under cubic symmetry operations, hence there are 48 identical monoclinic solutions, corresponding to the 8 symmetry related directions of polarization in each of the 6 $\{110\}$ planes. That is, monoclinic perovskite ferroelectrics have 48 degenerate domain states. On this basis, poling of monoclinic ceramics, would result in orientation of the favourable [111]-[001] channel in the (110) plane within the quadrant containing the poling direction and allowing the maximum piezoelectric contribution of polarization rotation in this plane. However, the nano-domains postulated in the Glazer model [26] are not locally degenerate. The implication is that the local Zr/Ti conformation biases the free energy function towards a specific direction of polarization. Poling may be able to switch the major component of polarization (i.e. along <111> or <001>). However, as the potential topology for each of the 48 domains states will be different, it is not clear what the effect on the minor components of cation displacement will be. Due to the "internal bias" provided by random Zr/Ti conformations, the contribution of polarization rotation in the (110) plane would be less significant than the symmetrical LGD model suggests and may be one reason why the predictions of Fig. 9 overestimate the piezoelectric coefficients. However, in the case of Zr/Ti ordering close to $z = 0.5$, in which a greater degree of local symmetry and domain state degeneracy might be restored, the polarization rotation model would be expected to be more significant.

9. Conclusions

Recently proposed models of piezoelectricity in morphotropic phase boundary perovskites and for the structure of PZT have been examined employing Landau-Ginzburg-Devonshire theory and statistical models of Zr/Ti conformation. It is shown that the mechanism of polarization rotation in the (110) plane can enhance the piezoelectric effect in ceramics and that the tendency towards the formation of macroscopic monoclinic forms facilitates this by reducing the energy for realignment of the polarization vector. The proposed model of static, monoclinic nano-domains which are observed as rhombohedral or tetragonal macroscopic structures appears to be consistent with the statistics of random Zr/Ti conformations across a large region of the PZT phase diagram. However, it is argued that the increase in coherence length of the nano-domains, proposed as the mechanism for the appearance of the macroscopic monoclinic phase close to $z = 0.5$, may be a consequence of some undetected order in the B-site cations. Furthermore, the biasing of the nano-domain orientation by the local Zr/Ti conformation may impede the polarization rotation contribution to the piezoelectric effect.

It has been argued that significant anisotropic thermal fluctuations, of the type that are seen in constrained structure refinements, are not inconsistent with the dielectric anisotropy of PZT, particularly under the assumption of a tendency towards macroscopic monoclinicity. This proposition would also be more consistent with the concept of significant polarization rotation and hence should not yet be ruled out in favour of the nano-domain structure model.

Further studies toward deeper insight are: structure determinations under applied electric fields; modelling of temperature factors from dielectric data; modelling of the switching of locally biased monoclinic domains; high resolution studies of Zr/Ti conformations at the MPB; a more

extensive study of the statistics of Zr/Ti conformations and larger scale *ab initio* simulations.

References

1. B. JAFFE, W. R. COOK and H. JAFFE, in "Piezoelectric Ceramics" (Academic Press Ltd, 1971).
2. Y. SAITO, H. TAKAO, T. TANI, T. NONOYAMA, K. TAKATORI, T. HOMMA, T. NAGAYA and M. NAKAMURA, *Nature* **432** (2004) 84.
3. S.-E. PARK and T. R. SHROUT, *J. Appl. Phys.* **82** (1997) 1804.
4. B. NOHEDA, D. E. COX, G. SHIRANE, J. A. GONZALO, L. E. CROSS and S. E. PARK, *Appl. Phys. Lett.* **74** (1999) 2059.
5. Z. G. YE, B. NOHEDA, M. DONG, D. COX and G. SHIRANE, *Phys. Rev. B* **64** (2001) 184114.
6. D. LA-ORAUTTAPONG, B. NOHEDA, Z. G. YE, P. M. GEHRING, J. TOULOUSE, D. E. COX and G. SHIRANE, *Phys. Rev. B* **65** (2002) 144101.
7. D. L. CORKER, A. M. GLAZER, R. W. WHATMORE, A. STALLARD and F. FAUTH, *J. Phys.- Cond. Matter,* **10** (1998) 6251.
8. D.-S. PAIK. S.-E. PARK, S. WADA, S.-F. LIU and T. R. SHROUT, *J. Appl. Phys.* **85** (1999) 1080.
9. H. FU and R. E. COHEN, *Nature* **403** (2000) 281.
10. A. J. BELL, *J. Appl. Phys.* **89** (2001) 3907.
11. A. F. DEVONSHIRE, *Adv. Phys.* **3** (1954) 85.
12. D. DAMJANOVIC, F. BREM and N. SETTER, *Appl. Phys. Lett.* **80** (2002) 652.
13. Z. WU and H. KRAKAUER, *Phys. Rev. B* **68** (2003) 014112.
14. N. HUANG, Z. LIU, Z. WU, J. WU, W. DUAN, B.-L. GU and X.-W. ZHANG, *Phys. Rev. Lett.* **91** (2003) 067602.
15. S. WADA, S. SUZUKI, T. NOMA, T. SUZUKI, M. OSADA, M. KAKIHANA, S.-E. PARK, L. E. CROSS and T. R. SHROUT, *Jpn. J. Appl. Phys.* **38** (1999) 5505.
16. J. F. NYE, in "Physical Properties of Crystals" (Oxford, 1985)
17. M. J. HAUN, E. FURMAN, S. J. JANG and L. E. CROSS, *Ferroelectrics* **99** (1989) 13.
18. M. J. HAUN, Z. Q. ZHUANG, E. FURMAN, S. J. JANG and L. E. CROSS, *ibid.* **99** (1989) 45.
19. X. DU, J. ZHENG, U. BELEGUNDU and K. UCHINO, *Appl. Phys. Lett.* **72** (1998) 2421.
20. D. V. TAYLOR and D. J. DAMJANOVIC, *ibid.* **76** (2000) 1615.
21. A. J. BELL, *ibid.* **76** (2000) 109.
22. D. VANDERBILT and M. H. COHEN, *Phys. Rev. B* **63** (2001) 4108.
23. J. FRANTTI, J. LAPPALAINEN, S. ERIKSSON, V. LANTTO, S. NISHIO, M. KAKIHANA, S. IVANOV and H. RUNDLOF, *Jpn. J. Appl. Phys.* **39** (2000) 5697.
24. A. J. BELL and E. FURMAN, *Ferroelectrics* **293** (2003) 29.
25. *Idem., Jpn. J. Appl. Phys. Pt. 1* **42** (2003) 7418.
26. A. M. GLAZER, P. A. THOMAS, K. Z. BABA-KISHI, G. K. H. PANG and C. W. TAI, *Phys. Rev. B* **70** (2004) 184123.
27. I. GRINBERG, V. R. COOPER and A. M. RAPPE, *Nature* **419** (2002) 909.
28. I. GRINBERG, V. R. COOPER and A. M. RAPPE, *Phys. Rev. B* **69** (2004) 144118.
39. A. J. BELL and P. GOUDOCHNIKOV, in "Proceedings of Material Technology and Design of Integrated Piezoelectric Devices", (2004) p. 29.
30. Y. M. JIN, Y. U. WANG, A. G. KHACHATURYAN, J. F. LI and D. VIEHLAND, *J. Appl. Phys.* **94** (2004) 3629.